Texturing edible oil with crystals of phenolic compounds: platelets versus rods

Authors: Angelo Pommella, Melody Mathonnat, Martin In

Affiliation: Laboratoire Charles Coulomb (L2C), Univ Montpellier, CNRS, Montpellier, France.

Corresponding author: martin.in@umontpellier.fr

Abstract

Cinnamic acid and acetosyringone recrystallize in vegetable oil as platelets and rods respectively. After dissolution at high temperature(100°C) and upon cooling down to room temperature, their crystallites aggregate into a tenuous network which spans the entire volume of the system even at low mass fraction such as 1%. The whole system behaves as a soft solid characterized by an elastic modulus reaching 1MPa for mass fraction ϕ below 10% in the linear regime. The elastic modulus of cinnamic acid based oleogels varies with mass fraction as $(\phi - \phi_0)^2$. For acetosyringone based oleogels, the elastic modulus varies non monotonically with concentration. This has been correlated to a morphological crossover from jammed spherulites at low mass fraction to entangled rods at higher mass fraction. Spherulite formation is related to the presence of branching points along the rods that result from secondary nucleation events. A new empirical parameter is defined from rheological data which reflects how far from equilibrium the solidification proceeds in non-isothermal conditions. This parameter accounts for the different concentration regimes of morphology and rheological properties that have been observed experimentally for acetosyringone.

Keywords

Rheology ; oleogelation ; crystallization ; non-TAG.

1. Introduction

The continuous incitement coming from government legislations and guidelines for a healthier nutrition has driven the food formulation away from trans and saturated fats. Trans and saturated triacylglycerol (TAG) usually introduced to improve the texture of fats, have been shown to increase the low density lipoproteins (LDL), commonly referred to as “bad cholesterol” that is responsible of cardiovascular diseases (WHO, 2003). Conversely, mono and polyunsaturated TAGs, from most vegetable oils are considered to lower LDL levels. From the nutrition point of view, it is strongly recommended to replace saturated fats with unsaturated ones (Rogers, 2009; Bot, Veldhuizen, den Adel & Roijers, 2009; Co & Marangoni, 2012; Patel & Dewettinck, 2015) but this is detrimental

regarding texture and specific mouth feel of food products because, at room temperature, saturated fats are solid while unsaturated ones are liquid. To achieve a suitable compromise between nutritional and textural properties of fats in food applications, the first step is to structure the unsaturated oil in a way or another, up to solidification if possible and with the lowest amount of additional solid compounds.

Organogelation is generically referred as the physical process allowing the solidification of oil without affecting its chemical properties (Daniel & Rajasekharan, 2003). At the end of the process, oils show a soft solid-like behaviour characterized by an equilibrium elastic modulus in the linear regime (Nayak & Das, 2018), but which can flow under harsher mechanical solicitation. This can be achieved by crosslinking of polymers (Dey, Kim & Marangoni, 2011; Davidovich-Pinhas, Barbut, & Marangoni 2016; Jiang et al., 2018) or aggregation of low-molar mass compounds called organogelators (Singh, Auzanneau & Rogers, 2017). Polymers and aggregates provide with the necessary connectivity to allow momentum transfer, but this connectivity has also to be limited so that the polymer or the aggregates spans the whole volume of the sample. To show structuring properties polymers must be soluble while aggregates must be tenuous and preferentially fractal. Research on the organogelation by low molar mass compounds has been driven by food applications (Gómez-Estaca et al., 2019; Rogers et al. 2014; Oh & Lee, 2018; Martins, Vicente, Cunha & Cerqueira, 2018; Tanti, Barbut & Marangoni, 2016a; Tanti, Barbut & Marangoni, 2016b) but a more general interest in structuring hydrophobic liquids using low-molecular weight organogelators is also found in waste oil disposal (Abdallah & Weiss, 2000a), oil spill remediation (Ohsedo, 2015), molecular delivery (O'Sullivan, Barbut & Marangoni, 2016), and pharmaceuticals (Ibrahim, Hafez & Mahdy, 2013). In food, organogelation also called oleogelation results more often from crystallization than from self-assembling. Self-assembling is an equilibrium process that offers less versatility in terms of processing parameters to control the final morphology of the aggregates, for instance the fractal dimension or the size of primary particles, while crystallization and subsequent aggregation of crystallites are far from equilibrium and depend strongly on how the crystal nucleation and growth of crystallites is carried on. Crystallization of alkanes (Abdallah & Weiss, 2000b), wax (Toro-Vazquez et al., 2007), fatty acids (Daniel & Rajasekharan, 2003), monoacylglyceride (MAG) (Batte, Wright, Rush, Idziak & Marangoni, 2007), phytosterols (Bot, Veldhuizen, den Adel & Roijers, 2009; Bot & Agterof, 2006), ceramides (Rogers, Wright & Marangoni, 2009), and proteins (Romoscanu & Mezzenga, 2006; de Vries, Jansen, van der Linden & Scholten, 2018) has been studied in the context of texturing edible oils. The art of texturing oil with low molar mass crystalline compounds is to avoid dense packing at large scale although dense packing at small scale is mandatory to build the primary solid particle. This is more conveniently achieved when crystals grow preferentially along one or two dimensions

leading to anisotropic primary particles. Some kinds of defects have to be present to hinder alignment of the rods or the platelets as to avoid dense packing. In literature, there are several studies on edible organogels made from needles- (Rogers, Wright & Marangoni, 2009; Kuwahara, Nagase, Endo, Ueda & Nakagaki, 1996; Kesselman & Shimoni, 2007) or platelet-like (Abdallah & Weiss, 2000b; Gandolfo, Bot & Flöter, 2004; Morales-Rueda, Dibildox-Alvarado, Charó-Alonso, Weiss & Toro-Vazquez, 2009) crystals but we do not know of any comparative study.

Here, we investigate the organogelation of sunflower oil with two different low-molecular weight organogelators, namely (2E)-3-Phenylprop-2-enoic referred to as cinnamic acid and 4'-Hydroxy-3',5'-dimethoxyacetophenone which will be referred to as acetosyringone. The concentration of phenolic compounds is the main varying parameter of this study. The chemical structure of these compounds is shown in Figure 1. They are two phenolic molecules already used as food additive (Adisakwattana, 2017) but not generally for their structuring properties. Cinnamic acid is a natural product commonly found in plants and known with its derivatives for their anti-diabetic (Hanhineva et al., 2010), antioxidant (Sova, 2012), anti-inflammatory (De Cássia da Silveira e Sá, Andrade, Dos Reis Barreto de Oliveira & De Sousa, 2014) and anti-cancer (Anantharaju, Gowda, Vimalambike & Madhunapantula, 2016) activity. It has recently been used as organogelator in rice bran oil (Li et al., 2017). Acetosyringone, another compound commonly found in plants (Baker et al., 2005; Agostini, Desjobert & Pergent, 1998), has never been studied for its oil structuring properties.

First the solubility of both compounds will be presented as a function of the temperature. Second, the kinetics of structuring induced by cooling at a fixed rate from high temperature down to 25°C will be reported. Once stabilized at 25°C the rheological properties of the systems are further characterized in the linear and in the non-linear regime. The concentration dependence of the organogel elasticity is found to be classical for cinnamic acid based organogels and corresponds asymptotically to a power law. However it is non-monotonous and unusual for acetosynringone base gels. A structural study by optical and electronic microscopy allows a tentative explanation for this unusual concentration dependence as due to the crossover from a regime of structuring by jamming of spherulites to a regime of structuring by rods entanglement.

2. Material and methods

2.1. Material

Acetosyringone (Aldrich, D134406-25G) and trans-cinnamic acid (Aldrich, W228818-1KG-K) have been used as received. Sunflower oil (Lesieur code 18205B03) has been bought from a grocery store and used as received.

2.2. Solubility determination

In a first series of experiments, various compounds have been screened according to the solubility differential between high temperature and low temperature. The screening process consist of heating 2g of sample in a 2ml glass vial at 3, 6 and 9% weight of the compounds in sunflower oil. The vials were put in an oven (Memmert E700) at 110°C, manually shaken from time to time until complete dissolution judged from visual observation. The vials were then brought out of the oven at room temperature and left at rest. It takes about one and half hours for the vial to be thermalized at room temperature, which corresponds to an average cooling rate of 1°C/min.

Solubility curves of both compounds were established by visual observation of the turbidity as temperature increases. Several suspensions of phenolic compound at different mass fractions from 1 to 12% in sunflower oil are prepared at room temperature. The suspensions are then heated up under magnetic stirring (Fischer Bioblock Scientific MR 3001K 800W with a regulation unit Heidolph EKT 3001). The temperature rise is carried on by steps of 1°C each lasting about ten minutes. When solid residues can no longer be detected, the dissolution is considered complete. The solubility curve presented below shows the mass fraction versus the lowest temperature of complete dissolution.

2.3 Rheology

Phenolic compound based oleogels were formed in between the rheometer parallel plates according to the following protocol : Suspensions of phenolic compound and sunflower oil were heated up to 110°C for acetosyringone or 100°C for cinnamic acid in suitable vials until complete dissolution. The hot clear solutions were then rapidly transferred onto the heated lower plate of the rheometer (Stress control Anton Paar MCR502) and the gap set to 1 mm. Sandblasted plates were used to avoid slip between the sample and the plates. A Peltier module (P-PTD200/56/I) controls the temperature of the measurement cell and cooling rate was set up at 10°C/min, down to the targeted temperature T_f=25°C. Time evolution of the rheological properties was monitored by dynamic oscillatory experiments at an angular velocity of 10 rad/s and a strain amplitude of 0.001% controlled by a feedback loop. In the course of gelation upon cooling the gap was adjusted in order to keep null the normal forces on the upper plate. Once the systems were stabilized, their rheological properties were further characterized at 25°C by dynamic oscillatory experiments, frequency sweep experiments in the linear regime and strain sweep experiments at an angular velocity of 10 rad/s.

2.4 Optical microscopy

Images of the organogels network were taken in bright field and in between crossed polarizers using an optical microscope Leica DMRX and a colour camera Thorlabs (DCC1645C) or a Nikon digital camera D5200. A low magnification objective 3.2X was used to visualize the network at large length scale. The organogels formed in vials under slow cooling condition or in the rheometer under faster cooling condition were gently transferred to a glass plate with a spatula.

To observe the structure under optical microscope without any transfer step, some organogels were prepared directly between a glass plate and a cover slide kept 150μm apart. The hot clear solution of acetosyringone or cinnamic acid in sunflower oil were prepared in the same way as for rheology experiments, it means hot clear solutions are introduced in a hot chamber (100°C for the cinnamic acid solutions and 110°C for the acetosyringone solutions). The filled chamber was then brought onto the microscope stage at room temperature for observation. The cooling was performed in uncontrolled but monitored conditions. The chamber thermalized within ten minutes corresponding to an average cooling rate of 7 to 8°C/min.

2.5. Scanning electron microscopy

Scanning electron microscopy (SEM) images of the organogel network were taken using a microscope FEI Quanta 200 FEG under high vacuum conditions. The organogel was gently transferred from the rheometer plates onto a piece of filter paper. The contact of the organogel with the filter paper partially drained out the oil from the samples by capillarity. Samples observed by SEM after such draining process still contained sunflower oil. To complete the removal of oil from the mesh of crystals, the drained organogel was transferred onto a new piece of filter paper and washed with cyclohexane. The use of organic solvent to condition fat sample for electronic microscope observation has been described previously and improve the resolution of observation (Heertje I, Leunis M, van Zeyl WJM, Berends E. 1987). The crystals were then dried on a piece of filter paper and left to evaporate for few minutes.

Both type of specimen, after draining and after washing, have been transferred to sample holder of the microscope and observed as extracted, without metallization.

3. Results and discussion

3.1. Solubility curve

Texturing oil by building up a crystalline network requires strong enough solubility differential between high and low temperature in order to allow reshaping of the solid by a heating-cooling cycle. The solubility of cinnamic acid and acetosyringone in sunflower oil shows a non-linear

dependence upon temperature (Figure2). Complete dissolution of 1% w/w cinnamic acid in sunflower oil is achieved at 51°C and at 60°C for 1w/w% of acetosyringone. At 99°C, up to 14.7% w/w of cinnamic acid can be dissolved and 12% w/w acetosyringone can be dissolved at 113°C. We did not exceed these temperatures to limit the oxidation of the oil. From Figure 2 we set to work in the mass fraction range from 1% to 7% in mass fraction for the acetosyringone and from 1% to 9% in mass fraction for the cinnamic acid.

3.2. Kinetics of gelation

The building up of the crystalline network in the oil upon cooling as monitored by the dynamic modulus is shown in Figure 3. The time evolution of the storage modulus *G** (black square) is reported on the left hand *y* axis. On the right hand y-axis is reported the decreasing temperature ramp (blue triangles) imposed to the sample after loading the sample between the plate. The origin of time is chosen as the onset of cooling. Initially the complex modulus fluctuates with large amplitudes around a mean value of 1Pa in both graphs of Figure 3. It is to recall that with the double plate geometry we used, the lowest modulus within the specification of the sensitivity range of the transducer of the rheometer is 10Pa. The time at which the complex modulus of the sample reaches 10Pa will be referred to as the structuring time and the corresponding temperature will be called the structuring temperature.

After an induction period, *G** increases suddenly and gets rapidly larger than 10Pa, reflecting the ongoing recrystallization of the phenolic compound upon cooling. For cinnamic acid at 3% (Figure 3a), *G** increase monotonically until the properties get stationary. For acetosyringone at 3.5% (Figure 3b), G* varies non monotonically and present an overshoot. This time evolution of the rheological properties of the acetosyringone based system is typical of intermediate mass fraction between 2 and 6%. Out of this concentration range, no overshoot was observed. The whole set of data of G* versus time during the structuring process is given in Figure SI 1 for all concentrations.

Figure 4 shows the structuring time t_s (black squares referring to the left *y* axis) and the structuring temperature T_s (blue triangles referring to the right *y* axis) as a function of the percentage of mass fraction ϕ. The structuring time t_s decreases as ϕ increases (Figure 4). The concentration dependence of the structuring time is stronger at low concentration than at high concentration. This has also been reported for the crystallization of cinnamic acid in rice bran oil (Li et al., 2017).

Two kinetic regimes can be distinguished both characterized by a power law dependence of the structuring time t_s upon concentration ϕ (Figure 4). For cinnamic acid based oleogels $t_s \sim \phi^{-12.4}$ for $\phi < 3\%$. For acetosyringone $t_s \sim \phi^{-3.3}$ for $\phi < 3\%$. At larger organogelator mass fractions ($\phi >$

192 3%), the mass fraction dependence of the gelation time becomes significantly weaker $t_s \sim \phi^{-1.4}$ for
193 cinnamic acid (Figure 4 a) and $t_s \sim \phi^{-0.9}$ for acetosyringone (Figure 4b). $\phi = 3\%$ corresponds also to
194 the mass fraction above which structuring occurs while temperature is still decreasing, whereas
195 below $\phi = 3\%$ the systems get solid after some time once the targeted temperature T_f has been
196 reached.

197 Strong concentration dependence of the gelation kinetics has been observed in many different
198 systems from proteins (Ross-Murphy, 1991) to ceramic gels (In & Prud'homme, 1993). For the
199 gelation kinetics of polymers the high apparent kinetic order has been interpreted in terms of the
200 competition between precipitation and gelation (de Gennes, 1979). Gelation kinetics show often
201 high apparent orders because dilution not only bring reactants further apart, but also because the
202 association process has to be brought further for gelation to occur. In chemical terms, we would say
203 that dilute conditions favour intramolecular bonds rather than intermolecular bonds and
204 intramolecular bonds consolidate the clusters but do not bring them closer to the gelation threshold,
205 so that more bonds to reach gelation. In physical terms, on the ground of the percolation model, it is
206 explained as an increase of the bond percolation threshold when the sites are correlated. The strong
207 power law dependence observed at low concentration in our systems (Figure 3) could be explained
208 by the fact that structuring and gelation occur through two combined processes which determines
209 the structure of the gels at different scales: crystal growth and aggregation (See Figure SI2).
210 Crystallization leads to dense ordered solid particles, and aggregation leads to tenuous random
211 clusters. As mentioned in the introduction, a necessary condition to form a gel from crystalline
212 compound is densely pack the molecules at small scale while avoiding dense packing at large scale in
213 order to span as large volume as possible. As concentration decreases, crystal growth proceeds more
214 slowly and leads to larger crystallites. Not only the kinetics of crystallization is slow down but also the
215 gelation threshold in terms of solid content might by be significantly increased and this possibly
216 explains the high apparent order of gelation kinetics.

217 ### 3.3. Linear and non-linear rheological properties of the organogels

218 The rheological properties of the organogels are presented in Figure 5, in both the linear and the
219 non-linear regime. They have been measured at 25°C, at the end of the time sweep experiments,
220 once the rheological properties got stationary. Frequency sweep experiments in the linear regime are
221 reported on the left hand side of Figure 5 while the right hand side presents the non-linear regime by
222 stress-strain curves. Upper graphs (a, b) are for organogels made with cinnamic acid and lower
223 graphs (c, d) report on acetosyringone based systems. Figure 5a shows the storage modulus *G'*
224 (square data) and the loss modulus *G''* (triangle data) of two cinnamic acid organogels at the mass

fraction of 2.5% (black data) and 9% (red data). In the range of frequency investigated, $G' > G''$ by more than one decade. Both moduli show a very weak dependence on the frequency if at all as pointed out by (Narine & Marangoni, 1999). In particular, no maximum is observed for the loss modulus which would have suggested a dissipation process associated with a particular time, nor a minimum which would have suggested different modes of dissipation at different time scale. The scattering of the G'' data at low frequency prevents to reliably infer the presence of a relaxation time at lower frequencies. At any accessible time, the system appears as a solid. The linear rheological behaviour of acetosyringone organogels presented in Figure 5c for two mass fractions, 1.5% (black data) and 7% (red data), is similar to the one of cinnamic acid.

The crossover from the linear to the non-linear regime is observed at very low strain for $\gamma \approx 0.01\%$ The log-log representation of the data from strain sweep experiments given Figure SI 3 are reminiscent of the one obtained on shortenings (Macias-Rodriguez, Marangoni, 2016). The non-linear shear strain dependence of the stress is shown in Figure 5b and 5d. This representation conveniently reflects the softening of the organogel, and the way $d\sigma/d\gamma$ decreases as γ increases from positive to negative values. For instance, such stress-strain curves at different mass fraction, evidence the progressive change of the organogels behaviour from ductile-like at low solid content (black data) to brittle-like at higher solid content (red data) as the maximum in the stress-strain curve gets more and more pronounced (Macias-Rodriguez, B. A.; Marangoni, A. A.2018)

3.4. Wettability of the crystals by sunflower oil.

The comparative study of the crystals by electron microscopy after draining the oil from the crystallite network or by rinsing with an organic solvent illustrates the wetting properties of the oil towards the solid phenolic compounds and reflects the interaction between the oil and the phenolic compounds. It is related to the oil binding capacity of the crystals (Yilmaz & Ögütcü, 2014; Giacomozzi, Palla, Carrin & Martini, 2019). In Figure 6, SEM images of acetosyringone organogels are presented, for different mass fractions of 1.2% (a, d), 1.5% (b, e) and 3.5% (c, f). Note that the samples have been recovered from rheology experiments and the structures observed have grown up in between the rheometer plates. The top micrographs in Figure 6 (a, b and c) have been recorded after simple drainage of the sunflower oil from the crystals with an adsorbing paper, while the micrographs at the bottom of Figure 6 (d, e, and f) have been recorded once oil was removed by rinsing the organogels with cyclohexane. Preliminary test had shown that cyclohexane was a good solvent for the oil and not for the phenolic compounds. Attempt to drain the oil out of organogel with the help of a filter paper challenges the oil retention capacity of the solid network. It measures the wetting capacity of the oil towards phenolic compounds, with reference to its wetting capacity

towards cellulosic solid. It is observed that a significant quantity of oil is retained by capillarity in the mesh of crystallites. For the lowest initial solid content, the details of the surface texture are not visible in Figure 6a, compared to the micrograph of Figure 6d obtained after rinsing with cyclohexane. The presence of a layer of oil that smears out the surface roughness shows the affinity of oil for the surface of the crystals. In more concentrated samples, enough oil is retained so that the crystalline rods of acetosyringone are no longer clearly visible as shown in Figure 6b and 6c. A salient feature of these micrographs is that the surface of the oil is no longer flat and smooth as expected for a liquid, but rather irregular, showing crest and peaks that are shaped by the tips of the acetosyringone needles that appear as white dots on the micrographs. This shows that the sample is no longer liquid and oil has been textured. Rinsing with cyclohexane reveals the details of the network of crystallites underneath (Figure 6e and 6f). It is made of entangled and branched rods. Such ability to interact and retain sunflower oil was found also in cinnamic acid crystals and it is essential to form an organogel where the oil represents the main component to be hold in the three-dimensional network.

3.5. Concentration dependence of the organogel elasticity.

In Figure 7, we show the dependence of the storage modulus on the organogelator mass fraction for the cinnamic acid (a) and acetosyringone (b) organogels. The elasticity of the sunflower oil textured by the phenolic compounds is in the same range found for anhydrous milk fat, canola oil and cocoa butter at solid fat content lower than 20% (Awad, Rogers & Marangoni, 2004), soft margarines, butter and various tablespreads at room temperature (Borwankar, Frye, Blaurock & Sasevich, 1992; Vithanage, Grimson & Smith, 2009) and flour batters (Renzetti, Dal Bello & Arendt, 2008). In addition, a similar range of elasticity is found for cosmetic products (Kwak, Ahn & Song, 2015). The level of elasticity of the sunflower oil structured by the present phenolic compounds is higher than the one obtained from polyconasol in olive oil (Lupi, Gabriele, Greco, Baldino, Seta, de Cindio, 2013) or monoglycerides in olive oil (Ojijo, Neeman, Eger & Shimoni, 2004), although it is worth mentioning that these systems were obtained at slower cooling rates.

Focusing on Figure 7a, we observe that the minimum mass fraction of cinnamic acid needed to form the organogel is 2% and the elastic modulus increases monotonically as mass fraction increases. The organogel elasticity shows a critical-like behaviour and can be fitted with the following equation:

$$G' = K \cdot (\phi - \phi_0)^{\alpha} \qquad \text{Equation 1}$$

with ϕ_0 the critical mass fraction, α the power-law exponent. Constraining ϕ_0= 2% leads to α = 2.0±0.1 and K =1.81·10^4 ± 100 Pa. Far from the critical mass fraction, for $\phi > \phi_0$, the elastic modulus scale as $G' \sim \phi^2$. In Figure 7b we report the dependence of the organogel storage modulus with the acetosyringone mass fraction. Here the minimum organogelator mass fraction required is 1%. In contrast with cinnamic acid system, the mass fraction dependence of the storage modulus is non-monotonic, showing a singular minimum around 3.5%. Such non-monotonic concentration dependence of the elastic properties suggests a qualitative change of structure correlated with the concentration regime.

Power law dependence of the elastic modulus upon solid content has been observed frequently in fat systems (Awad, Rogers & Marangoni, 2004 ; Ojijo, Neeman, Eger & Shimoni, 2004 ; Lupi, Gabriele, Greco, Baldino, Seta, de Cindio, 2013). It is a characteristic feature of randomly aggregated colloidal systems and the exponent has been theoretically related to the fractal dimension of the aggregates by modelling the whole system as a closed packed ensemble of fractal flocs or microstructural elements (Shih, Shih, Kim, Liu & Aksay, 1990 ; Narine & Marangoni, 1999, and references therein). An essential point of this model is that the elastic constant of a fractal flocs depends on its size. Two regimes have been distinguished depending on the fact that the stress is carried by the internal structure of the flocs or by the junctions between them. In the weak link regime expected for high volume fractions, the flocs should be small and characterized by a high elastic constant, so they do not deform easily, and only the link between flocs are bent upon strain and carry the stress. In the strong link regime expected for low volume fraction, the flocs are large and more compliant and deform upon strain (Shih, W. H., Shih, W. Y., Kim, S. I., Liu J. & Aksay, I. A., 1990). The exponent α characterizing the volume fraction dependence of the elastic modulus, $G' \sim \phi^{\alpha}$, is expected to be smaller in the weak link regime where it reads :

$$\alpha_w = \frac{1}{3-D} \qquad \text{Equation 2}$$

than in the strong link regime where it reads:

$$\alpha_s = \frac{3+x}{3-D} \qquad \text{Equation 3}$$

Where x is the fractal dimension of the backbone of the floc and varies between 1 and 1.3.

For the cinnamic acid based system, the low value of the exponent, α = 2.0±0.1, suggests that the oleogels are in the weak link regime despite the fact that we are at quite low volume fraction. The corresponding fractal dimension is D=2.5 and falls within the range classically observed in fat (Narine & Marangoni, 1999; Awad, Rogers & Marangoni, 2004 ; Lupi, Gabriele, Greco, Baldino, Seta, de

Cindio, 2013). Assuming a strong link regime and applying Equation 3 with x values between 1 and 1.3 leads to unacceptable values of the fractal dimension equal or lower than 1.

For the acetosyringone based system, the presence of a minimum of *G'* (Figure 7b) indicates that the acetosyringone organogel does probably not develop as a unique type of fractal network over the whole concentration range and the decrease of elasticity observed in a narrow range of concentration probably reflects a transition to which the next section is dedicated.

3.6. Morphology of crystals and its dependence on the process.

First, the morphology of crystals obtained at 3% under slow cooling conditions in vials (as explained section 2.2) is observed by optical microscopy under crossed polarizers (Figure 8a and 8b). It is worth noting that in these conditions of cooling and in such containers, 3% w of the phenolic compounds led to large crystals formation at the bottom of the vial. Crystals appear bright and coloured, consistent with their known anisotropic crystalline structure which is responsible for their birefringence. Acetosyringone cystals are tetragonal l41cd according to (He & yang, 2009) and trans-cinnamic acid crsytals are monoclinic P21/n according to (Ladell, McDonald & Schmidt, 1956 ; Schmidt 1964). The crystal structure of both phenolic compounds show that they solidification relies on hydrogen bonding and π-π stacking interactions, which is a general feature of phenolic compounds (Seth , Sarkar, Roy & Kar, 2011) and molecular organogels (Rogers, Strober, Bot, Toro-Vazquez, Stonz & Marangoni, 2014,). Cinnamic acid crystals are platelet-like shape and connect each other mainly by face-to-face or face-to-edge interactions. Here, face-to-face interactions form stacks of several platelets with different thickness that generate mosaics of different colours (top-centre of the image). Conversely, the face-to-edge interactions can be observed in particular between single platelets (or stacks of few platelets) with similar thickness and characterized by a uniform white colour as shown by the small mostly white part on upper left area of Figure 8a. Figure 8b shows that under slow recrystallization conditions acetosyringone leads to a network of entangled needle-like crystals that looks very different from the curved and branched structures formed in the rheometer under rapid cooling conditions (Figure 6). This result suggests that the structure of Figure 8b may not be present in the entire mass fraction range investigated due to the different conditions of the organogel formation.

Observations by optical microscopy of organogels obtained at different mass fractions after rapid cooling are presented in Figure 9 for acetosyringone and in Figure SI4 for cinnamic acid. After rapid cooling conditions the optical texture of cinnamic acid based oleogel does not show rigid platelets as the ones observed after slow cooling in Figure 8a. Instead, at 2% weight fraction (Figure SI4a)

crystallites appear as undulated ribbons of up to a few tens of microns wide and up to a few hundreds of microns long. The ribbons are loosely aggregated and form a 3D network with large voids. The observations presented in Figure SI4a are similar to those reported for cinnamic acid recrystallized in rice bran oil (Li et al., 2017). At 4% and 8% characteristic length of the optical texture decreases to 50μm and 40μm respectively (Figure SI4 b and c) but details on the morphology of the crystallites are not resolved. SEM images of cinnamic acid crystals (Figure SI5) show stacks of platelets at 7 and 9%.

The upper images of Figure 9a-d were recorded with an optical microscope and correspond to crystals organogels obtained upon fast cooling between a glass plate and a cover slide kept 150μm apart (Figure 9a-d). The images presented at the bottom of Figure 9 (e-f) were recorded with a smartphone camera and show the textured sunflower oil on the bottom plate of rheometer, after the time sweep experiments presented in Figure 3. For 1.2% of acetosyringone, large, curved and branched rod-like crystallites are observed in Figure 9a and Figure 9e and, similarly to Figure 6d, with a millimetric length and a thickness of tens of μm. The distance between two branching points is estimated at about 200 μm or larger from Figure 9e. This image at larger scale also evidences the tree-like structure of the crystallites and show well separated low density spherulites. At 1.5%, smaller and thinner branched rods are observed at the microscopic scale (Figure 9b), the distance between two branching points decreased down to about 100 μm and for this higher mass fraction, the tree-like structure is now evidenced at the microscopic scale and no longer at macroscopic scale (Figure 9f) due to overlap of the spherulites. At 3.5% of acetosyringone the spherulites are evidenced at the microscopic scale but rods and branching points are respectively too thin and too close to each other to be distinguished at this resolution. High density of branching points and overcrowding of the spherulites make the organogel opaque and smears out the contrast at the macroscopic level (Figure 9g). Last, at 7% a qualitative change in the network structure is observed: At the microscopic scale, long and straight rods are observed (Figure 9d) reminiscent of what was observed upon slow recrystallization in Figure 8b and at the macroscopic scale the sample is less opaque (Figure 9h). The fact that features are successively observed at macroscale and then at microscale in Figure 9, points out a decrease of two characteristic lengths of the network as concentration increases, namely the thickness of the rods and of the distance between branching points. The thinning of the rods as well as the increasing density of branching points are related to the kinetics of crystallization and the level of supersaturation, which controls the primary and secondary nucleation rate, which in turn determines respectively the number of spherulites and the degree of branching.

The non-monotonic concentration dependence of the rheological properties of the organogels shown in Figure 7b, can now be interpreted in terms of structure. At low concentration, the elasticity

comes from the overlap of spherulites formed by the tree-like structure of the crystal. As concentration increases, the number of spherulites increases due to the increase in primary nucleation rate but also branching density increases due to the increase in secondary nucleation rate.

The increase of the primary nucleation rate leads to an increase in the number of spherulites and a thinning of the rods because a higher number of nucleation points generate more crystals in the solution. This effect explains the thinning of the rods observed in the acetosyringone organogels varying the concentration from 1.2% to 3.5% and the decrease of the size of the platelets in the cinnamic acid organogels.

Branching results from secondary nucleation : The surface of already grown crystal favours new nucleation events and, depending on the supersaturation level of the system, the crystallographic orientation of the secondary nuclei can be different than the one of the pre-existing crystal. The higher the supersaturation level, the more chance to get different orientations because the mismatch constitutes a nucleation barrier to be overcome (Wang, Liu, Narayanan, Xiong & Li, 2006). Secondary nucleation is evidenced in Figure 6d and Figure 9a as sort of indentations on the curved rods. Figure 2 in SI shows that these indentations are in fact several grown crystals with different orientations. Branching contributes more to the densification of the spherulites than to their spatial expansion. This reduces the overlapping of spherulites and probably explains the decrease of elasticity as concentration increases, in the low concentration range. In the high concentration range, Φ > 3.5%, branching is no longer observed and the elasticity of the system results from the entanglement between long straight rods and it is determined by the mesh size of the network which decreases as concentration increase. Note that in the case of entanglements, the decreases of the characteristic mesh size of the network is no longer an effect of the kinetics of crystallization but a simple geometrical consequence of the increase in volume fraction, provided the cross section of the rods is constant.

It remains to explain why branching no longer occurs at high concentration (figure 9d), as if the supersaturation level would decrease while the concentration increases. But in practice we do not know the surpersaturation along the crystallization process because we could not monitor solid content of the sample. To compensate for this lack of information when relying solely on rheological experiments, we propose to characterize the whole solidification process by a single parameter $\sigma(\phi)$ calculated for each mass fraction ϕ, using the following relation:

$$\sigma(\phi) = (T^*(\phi) - T_S)/T^*(\phi) \qquad \text{Equation 4}$$

$T^*(\phi)$ is the temperature of complete solubilisation at a weight fraction ϕ. It is obtained from the solubility curve presented in Figure 2. T_S is the structuring temperature given in Figure 4. The

parameter $\sigma(\phi)$ reflects in a semi-quantitative way how far from equilibrium did the crystallization take place. This parameter takes into account both the thermodynamic of solubility of the compound through $T^*(\phi)$ but also the kinetic aspects of the process because T_S depends on the cooling rate. On the other hand, this parameter is built from temperature values and in a similar wayas a supercooling degree. But it should not be understood as a supercooling degree since we are dealing with recrystallization in a solvent under non-isothermal condition.

Figure 10 shows that $\sigma(\phi)$ varies non monotonically for the cinnamic acid (a) and acetosyringone (b) and goes through a maximum. The maximum found at ϕ =5% for cinnamic acid and at ϕ =3% for acetosyringone, corresponds to the concentration below which T_S is equal to the targeted temperature T_f=25°C. The increasing part of the $\sigma(\phi)$ curve is just a translation of the solubility curve and reads:

$$\sigma(\phi) = 1 - 298/T^*(\phi) \qquad \text{Equation 5}$$

In the present study, the cooling rate was fixed at 10°C/min, and cinnamic acid has been recrystallized in conditions where σ varies from 0.10 to 0.16, while the conditions of acetosyringone recrystallization cover a broader range of σ from 0.04 to 0.18. Also worth to notice on the graph of $\sigma(\phi)$ for the acetosyringone (Figure 9, red data), is the sharp maximum observed at Φ=3% which is close to the sharp minimum observed for the concentration dependence of the elasticity presented in Figure 7b.

The parameter $\sigma(\phi)$ seems to capture the different concentration regimes evidenced by rheology and structural observation in the case of acetosyringone. At low mass fraction, for Φ<3% , the increase of $\sigma(\phi)$ is correlated with the increasing internal density of spherulites and the number density of branching points as observed for the lowest concentrations in Figure 9. At high concentration, $\sigma(\phi)$ decreases down to values lower than the ones corresponding to lowest concentration and that could explain why no branching occurs at the highest concentration. The newly defined parameter addresses the apparent contradiction raised by the fact that defect free crystallites were obtained at the highest concentration. In non-isothermal condition, cooling rate counts as much as concentration and the parameter $\sigma(\phi)$ provides a simple way to assess qualitatively on the level of supersaturation simply from rheological measurements.

For cinnamic acid the amplitude of supercooling degree might not be large enough to translate into several concentration regimes and the concentration dependence of the rheological properties is regular.

The possibility of using a simply determined parameter such as $\sigma(X)$ to tune the organogel structure is important to modulate the rheological properties of organogels by varying independently the organogelator concentration or the cooling rate. For example, in the acetosyringone organogel, a more elastic organogel made of a fibrillar network could be obtained also at intermediate concentrations (e.g. 3.5%) by changing the operative conditions of the organogelation like the system cooling rate (Li, Yuan, Liu, R.-Y. Wang & X.-G. Wang, 2013). Using a lower cooling rate allows one to increase *T** reducing the supercooling conditions and, consequently, a fibrillar network is made at the same concentration. We found that this can be done only with organogels made of needle-like crystals of acetosyringone in the range of supercooling explored while larger supercooling conditions not always easily accessible (e.g. faster cooling rate) might be needed for organogels made of platelet-like crystals in order to induce different networks. Therefore, the choice of the crystal shape should be carefully evaluated to make an organogel and needle- or platelet-like crystals can be used depending on the applications. Needle-like crystals could be used when constraints on the organogelator concentration or on the temperature gelation are present whereas platelet-like crystals can be used when it is not possible to control carefully the system supersaturation due to its lesser effect on the system.

5. Conclusions

In the present study two phenolic compounds that crystallize either as rods or platelets have been shown to texture sunflower oil. The shape of the crystallites makes no qualitative difference in terms of the rheological properties (frequency dependence of the dynamic modulus and extent of linear regime). Both systems are similar to granular pastes: their solid building units are rather large, they are elastic at very low strain but soften at high strain. Without any optimization of the cooling process, the level of elasticity reached with these new systems is in the range 10^3 – 10^6 Pa, which is suited for food application. The texturing ability of the phenolic compounds is related to the tenuous structure of the aggregates of crystallites and to the wettability of these compounds by the sunflower oil.

The concentration dependence of the rheological properties is very different between the rods and the platelets system. Cinnamic acid organogels show ribbons or platelet aggregation as in a house of cards structure. The main effect of increasing the concentration in the platelet system is to reduce the size of the crystallite. On the other hand, in acetosyringone based rods system, in addition to a decrease in the characteristic dimensions, a qualitative change of the structure from jammed spherullites to entangled rods is evidenced as concentration increases. This is associated to the disappearance of branching points which result from secondary nucleation induced defects. We

484 define a parameter σ which reflects how deep in the unstable region of the phase diagram the
485 texturing process takes place. It accounts well with regards to its simplicity, for the various
486 concentrations regimes observed and could be a useful indicator for process optimization.

487 This study confirms the interest of phenolic compounds as alternatives for saturated or trans-TAGs
488 for texturing edible oils. Building a solid tenuous network from such compounds no longer relies on
489 van der Waals interactions but also on hydrogen bonds or π-stacking interactions. The nature of
490 phenolic compounds and the variety of their structure allow reasonable solubility at high
491 temperature and offer large variety of crystals habits. Phenolic compounds could improve the
492 nutritional value of food products not only through the reduction of saturated TAG proportion in the
493 formulation, but could also bring additional health or storage benefits due to their antioxidant
494 activity. The recrystallization of cinnamic acid and acetosyringone has also been observed in
495 rapeseed oil, although not reported here, leading to similar textures. However, to definitively assert
496 on the texturing capacity of such compounds, further studies, more focused on specific targeted
497 applications are needed and optimization of processing protocols would be required, with faster
498 cooling rate. From the basic point of view, structural studies of the crystalline phases obtained in oil
499 and thermodynamic studies of solubility are on going.

500 ## 6. Conflicts of interest

501 The authors declare no conflict of interest.

502 ## 7. Acknowledgements and funding

503 AP and MM thank the SAS PIVERT for funding. This work was performed, in partnership with the SAS
504 PIVERT, within the frame of the French Institute for the Energy Transition (Institut pour la Transition
505 Energétique (ITE) P.I.V.E.R.T. (www.institut-pivert.com) selected as an Investment for the Future
506 ("Investissements d'Avenir"). This work was supported, as part of the Investments for the Future, by
507 the French Government under the reference ANR-001-01

508 ## 8. References

509 Abdallah, D. J., Weiss, R. G. (2000a). **Organogels and Low Molecular Mass Organic Gelators.** *Adv.*
510 *Mater., 12, 1237-1247.*

511 Abdallah, D. J., Weiss, R. G. (2000b). **n-Alkanes Gel n-Alkanes (and Many Other Organic Liquids).**
512 *Langmuir, 16, 352-355.*

513 Adisakwattana, S (2017). **Cinnamic Acid and Its Derivatives: Mechanisms for Prevention and**
514 **Management of Diabetes and Its Complications.** *Nutrients, 9, 163.*

Agostini, S., Desjobert, J.-M., Pergent, G. (1998). **Distribution of phenolic compounds in the seagrass Posidonia oceanica.** *Phytochemistry, 48, 611-617.*

Anantharaju, P. G., Gowda, P. C., Vimalambike, M. G., Madhunapantula, S. V. (2016). **An overview on the role of dietary phenolics for the treatment of cancers.** *Nutr. J., 15, 99.*

Awad, T.S., Rogers, M. A., Marangoni, A.G. (2004). **Scaling Behavior of the Elastic Modulus in Colloidal Networks of Fat Crystals.** *J. Phys. Chem. B, 108, 171-179.*

Baker, C. J., Mock, N. M., Whitaker, B.D., Roberts,D. P., Rice, C. P., Deahl, K. L., Aver'yanov, A. A. (2005). **Involvement of acetosyringone in plant–pathogen recognition.** *Biochem. Biophys. Res. Commun., 328, 130-136.*

Batte, H. D., Wright, A. J., Rush, J. W., Idziak, S. H. J., Marangoni, A. G. (2007). **Phase Behavior, Stability, and Mesomorphism of Monostearin–oil–water Gels.** *Food Biophys., 2, 29–37.*

Borwankar, R. P. , Frye, L. A., Blaurock, A. E., Sasevich, F. J. (1992). **Rheological characterization of melting of margarines and tablespreads.** *J. Food Eng., 16, 55-74.*

Bot, A., Agterof, W. G. M. (2006). **Structuring of edible oils by mixtures of γ-oryzanol with β-sitosterol or related phytosterols.** *J. Am. Oil Chem.' Soc., 83, 513–521.*

Bot, A., Veldhuizen, Y. S. J., den Adel, R., Roijers, E. C. (2009). **Non-TAG structuring of edible oils and emulsions.** *Food Hydrocoll., 23, 1184-1189.*

Co, E. D., Marangoni, A. G. (2012). **Organogels: An Alternative Edible Oil-Structuring Method.** *Journal J. Am. Oil Chem.' Soc., 89, 749–780.*

Daniel, J., Rajasekharan, R. (2003). **Organogelation of plant oils and hydrocarbons by long-chain saturated FA, fatty alcohols, wax esters, and dicarboxylic acids.** *J. Am. Oil Chem.' Soc., 80, 417–421.*

Davidovich-Pinhas, M.; Barbut, S.; Marangoni, A. G. (2016) **Development, Characterization, and Utilization of Food-Grade Polymer Oleogels.** In *Annual Review of Food Science and Technology*, Vol 7, Doyle, M. P.; Klaenhammer, T. R., Eds. pp 65-91.

de Cássia da Silveira e Sá, R., Andrade, L. N., Dos Reis Barreto de Oliveira, R., de Sousa, D. P. (2014). **A Review on Anti-Inflammatory Activity of Phenylpropanoids Found in Essential Oils.** *Molecules, 19, 1459-1480.*

de Gennes, P. G. (1979). **Scaling Concepts in Polymer Physics.** Ithaca, Cornell University Press, (Chapter V).

de Vries, A., Jansen, D., van der Linden, E., Scholten, E. (2018). **Tuning the rheological properties of protein-based oleogels by water addition and heat treatment.** *Food Hydrocoll., 79, 100-109.*

Dey, T., Kim, D. A., Marangoni, A. G. (2011) **13 - Ethylcellulose Oleogels.** In *Edible Oleogels* (pp 295-311). AOCS Press.

Gandolfo, F. G., Bot, A., Flöter, E. (2004). **Structuring of edible oils by long-chain FA, fatty alcohols, and their mixtures.** *J. Am. Oil Chem.' Soc., 81, 1–6.*

Giacomozzi, A. S., Palla, C. A., Carrin, M. E. & Martini, S. (2019), **Physical Properties of Monoglycerides Oleogels Modified by Concentration, Cooling Rate, and High-Intensity Ultrasound.** *J. Food Science 2019, 84, 2549-2561.*

Gómez-Estaca, J., Herrero, A. M., Herranz, B., Álvarez, M. D., Jiménez-Colmenero, F., Cofrades, S. (2019). **Characterization of ethyl cellulose and beeswax oleogels and their suitability as fat replacers in healthier lipid pâtés development.** *Food Hydrocoll., 87, 960-969.*

Hanhineva, K. Törrönen, R., Bondia-Pons, I. Pekkinen, J., Kolehmainen, M., Mykkänen, H., Poutanen, K. (2010). **Impact of Dietary Polyphenols on Carbohydrate Metabolism.** *Int. J. Mol. Sci., 11, 1365–1402.*

He, J., Yang, J.-C. (2009). **1-(4-Hydroxy-3,5-dimethoxyphenyl)ethanone.** Acta Cryst. E*, 65, o3030.*

Heertje I, Leunis M, van Zeyl WJM, Berends E. 1987. **Product microscopy of fatty products***. Food Microstruct., 6, 1–8.*

Ibrahim, M. M., Hafez, S. A., Mahdy, M. M. (2013). **Organogels, hydrogels and bigels as transdermal delivery systems for diltiazem hydrochloride.** *Asian J. Pharm. Sci., 8, 48-57.*

In, M., Prud'homme, R. K. (1993). **Fourier transform mechanical spectroscopy of the sol-gel transition in zirconium alkoxide ceramic gels.** *Rheol. Acta, 32, 556–565.*

Jiang, Y., Liu, L., Wang, B., Sui, X., Zhong, Y., Zhang, L., Mao, Z., Xu, H. (2018). **Cellulose-rich oleogels prepared with an emulsion-templated approach.** *Food Hydrocoll., 77, 460-464.*

Joly-Duhamel, C., Hellio, D., Ajdari, A., Djabourov, M. (2002). **All Gelatin Networks: 2. The Master Curve for Elasticity.** *Langmuir, 18, 7158-7166.*

Kesselman, E., Shimoni, E. (2007). **Imaging of Oil/Monoglyceride Networks by Polarizing Near-Field Scanning Optical Microscopy.** *Food Biophys., 2, 117–123.*

T. Kuwahara, T., Nagase, H., Endo, T., Ueda, H., Nakagaki, M. (1996). **Crystal Structure of DL-12-Hydroxystearic Acid.** *Chem. Lett., 25, 435-436.*

Kwak, M.-S., Ahn, H.-J., Song K.-W. (2015). **Rheological investigation of body cream and body lotion in actual application conditions.** *Korea-Aust. Rheol. J., 27, 241–251.*

Ladell, J., McDonald, T. R. R., Schmidt, G. M. J. (1956). **The crystal structure of [alpha]-trans-cinnamic acid.** *Acta Cryst., 9, 195.*

Li, J.-L., Yuan, B., Liu, X.-Y., Wang, R.-Y., Wang, X.-G. (2013). **Control of crystallization in supramolecular soft materials engineering.** *Soft Matter, 9, 435-442.*

Li, X., Saleh, A. S. M., Wang, P., Wang, Q., Yang, S., Zhu, M., Duan, Y., Xiao, Z. (2017). **Characterization of Organogel Prepared from Rice Bran Oil with Cinnamic Acid.** *Food Biophys., 12, 356–364.*

Lupi, F. R., Gabriele, D., Greco, V., Baldino, N., Seta, L., de Cindio, B. (2013) **A rheological characterisation of an olive oil/fatty alcohols organogel.** *Food Research International, 51, 510-517.*

Macias-Rodriguez, B.; Marangoni, A. G. (2016). **Rheological characterization of triglyceride shortenings**. *Rheologica Acta*, *55*, 767-779

Macias-Rodriguez, B. A. and Marangoni, A. A. (2018). **Linear and nonlinear rheological behavior of fat crystal networks**. *Critical Reviews in Food Science and Nutrition, 58, 2398-2415*.

Martins, A. J., Vicente, A. A., Cunha, R. L., Cerqueira, M. A. (2018). **Edible oleogels: an opportunity for fat replacement in foods.** *Food Funct., 9, 758-773.*

Morales-Rueda, J. A., Dibildox-Alvarado, E., Charó-Alonso, M. A., Weiss, R. G., Toro-Vazquez, J. F. (2009). **Thermo-mechanical properties of candelilla wax and dotriacontane organogels in safflower oil.** *Eur. J. Lipid Sci. Technol., 111, 207-2015.*

Narine, S. S., Marangoni, A. G. (1999), **Relating structure of fat crystal networks to mechanical properties: a review**. *Food Research International, 32, 227-248.*

Nayak, A. K., Das, B. (2018) **Introduction to polymeric gels.** In K. Pal & I. Banerjee (Eds), *Polymeric Gels* (pp 3-27). Woodhead Publishing.

Oh, I. K., Lee, S. (2018). **Utilization of foam structured hydroxypropyl methylcellulose for oleogels and their application as a solid fat replacer in muffins.** *Food Hydrocoll., 77, 796-802.*

Ojijo, N. K., Neeman, I., Eger, S., Shimoni, E. (2004) **Effects of monoglyceride content, cooling rate and shear on the rheological properties of olive oil/monoglyceride gel networks**. *J. Sci. Food Agric., 84, 1585-1593.*

Ohsedo, Y. (2015). **Low-molecular-weight organogelators as functional materials for oil spill remediation.** *Polym. Adv. Technol., 27, 704-711.*

O'Sullivan, C. M., Barbut, S., Marangoni, A. G. (2016). **Edible oleogels for the oral delivery of lipid soluble molecules: Composition and structural design considerations.** *Trends Food Sci. Technol., 57, 59-73.*

Patel, A. R., Dewettinck, K. (2015). **Edible oil structuring: an overview and recent updates.** *Food Funct., 7, 20-29.*

Renzetti, S., Dal Bello, F., Arendt, E. K. (2008). **Microstructure, fundamental rheology and baking characteristics of batters and breads from different gluten-free flours treated with a microbial transglutaminase.** *J. Cereal Sci., 48, 33-45.*

Romoscanu, A. I., Mezzenga, R. (2006). **Emulsion-Templated Fully Reversible Protein-in-Oil Gels.** *Langmuir, 22, 7812-7818.*

Rogers , M. A.(2009). **Novel structuring strategies for unsaturated fats – Meeting the zero-trans, zero-saturated fat challenge: A review.** *Food Res. Int., 42, 747-753.*

Rogers, M. A., Wright, A. J., Marangoni, A. G. (2009). **Oil organogels: the fat of the future?** *Soft Matter, 5, 1594-1596.*

Rogers, M. A., Strober, T., Bot, A., Toro-Vazquez, J. F., Stortz, T., Marangoni, A. G.(2014). **Edible oleogels in molecular gastronomy.** *Int. J. Gastron. Food Sci., 2, 22-31.*

Ross-Murphy, S. B. (1991) **Concentration Dependence of Gelation Time.** In E. Dickinson (1st Eds), *Food Polymers, Gels and Colloids* (pp 358-368). Woodhead Publishing.

Schmidt, G. M. J. (1964) **Topochemistry III. Crystal chemistry of some trans-cinnamic acids**, *J. Chem. Soc. 2014-2021.*

Seth, S. K.; Sarkar, D.; Roy, A.; Kar, T. (2011) **Insight into supramolecular self-assembly directed by weak interactions in acetophenone derivatives: crystal structures and Hirshfeld surface analyses**. *Crystengcomm 13, 6728-6741*.

Singh, A., Auzanneau, F. I.& Rogers M. A. (2017) **Advances in edible oleogel technologies - A decade in review**. Food Research International, 97, 307-317.

629 Sova, M. (2012). **Antioxidant and Antimicrobial Activities of Cinnamic Acid Derivatives.** *Mini-Rev.*
630 *Med. Chem., 12, 749-767.*

631 Tanti,R., Barbut, S., Marangoni, A. G. (2016a). **Oil stabilization of natural peanut butter using food**
632 **grade polymers.** *Food Hydrocoll., 61, 399-408.*

633 Tanti,R., Barbut, S., Marangoni, A. G. (2016b). **Hydroxypropyl methylcellulose and methylcellulose**
634 **structured oil as a replacement for shortening in sandwich cookie creams.** *Food Hydrocoll., 61, 329-*
635 *337.*

636 Toro-Vazquez, J. F., Morales-Rueda, J. A., Dibildox-Alvarado, E., Charó-Alonso, M., Alonzo-Macias, M.,
637 González-Chávez, M. M. (2007). **Thermal and Textural Properties of Organogels Developed by**
638 **Candelilla Wax in Safflower Oil.** *J. Am. Oil Chem.' Soc., 84, 989–1000.*

639 Vithanage, C. R., Grimson, M. J., Smith, B. G. (2009). **The effect of temperature on the rheology of**
640 **butter, a spreadable blend and spreads.** *J. Texture Stud., 40, 346–369.*

641 Wang, R.-Y., Liu, X.-Y., Narayanan, J., Xiong, J.-Y., Li, J.-L. (2006). **Architecture of Fiber Network: From**
642 **Understanding to Engineering of Molecular Gels.** *J. Phys. Chem. B, 110, 25797-25802.*

643 World Health Organization (2003). **Diet, nutrition and the prevention of chronic diseases.** *WHO*
644 *Technical Report Series 916.*

645 Yilmaz, E., & Ögütcü, M. (2014). **Properties and stability of hazelnut oil organogels with beeswax**
646 **and monoglyceride**. *J. Am. Oil Chem.' Soc., 81, 1–6., 91, 1007- 1017.*

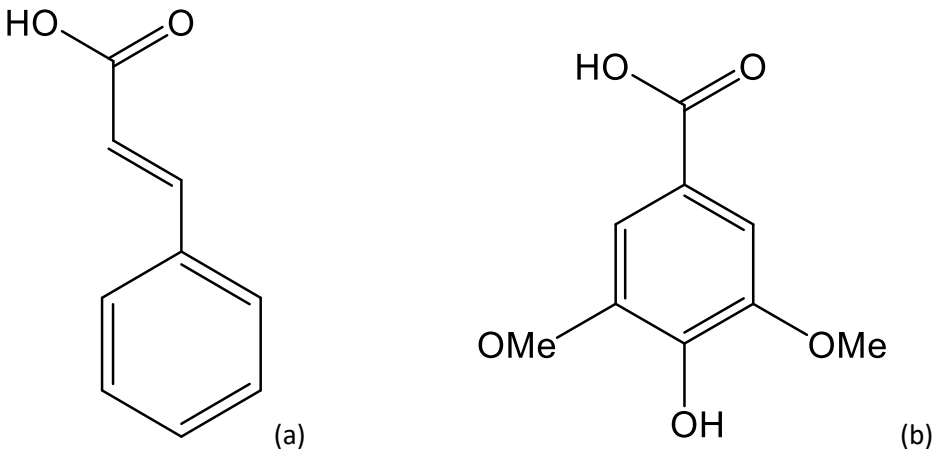

Figure 1 - Chemical structure of Cinnamic acid (a); Acetosyringone (b).

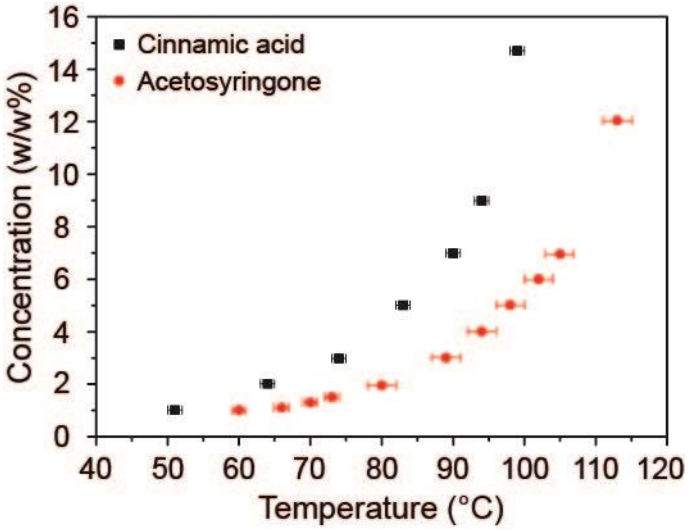

Figure 2 - Solubility curve of the cinnamic acid (■) and the acetosyringone (●) in sunflower oil.

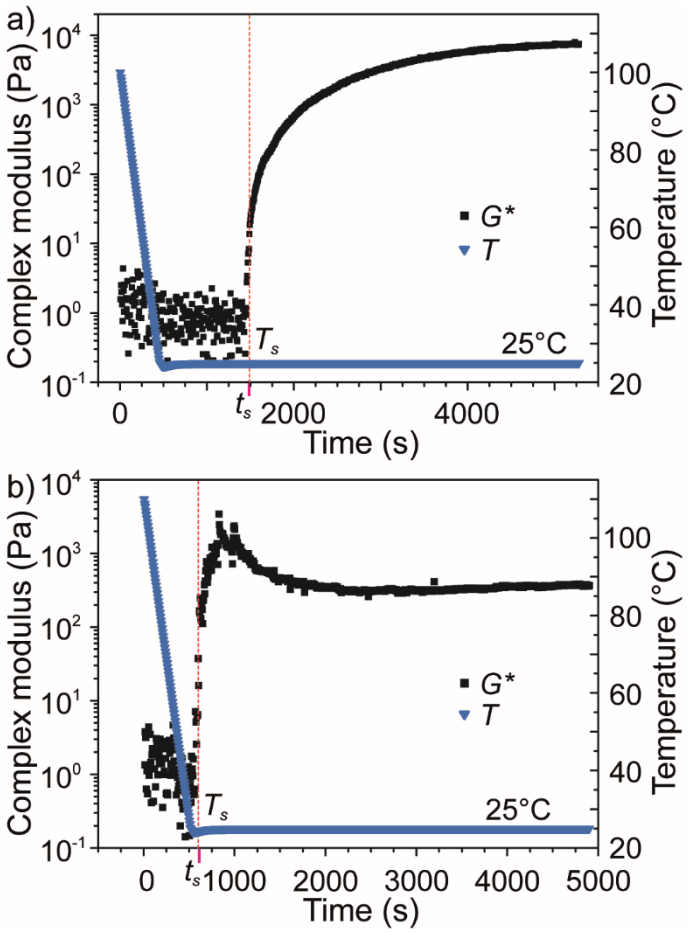

Figure 3 – Texturing sunflower oil by cinnamic acid at 3% (a) and acetosyringone at 3.5% (b) : Complex modulus G* (left y axis) versus time, upon cooling at 10°C/min. The temperature is presented on the right y axis. The time at which G* > 10 Pa is referred to as the structuring time t_s (pointed out on the graph by a dotted vertical line). The corresponding temperature will be referred to as the structuring temperature T_S. The moduli are measured at a frequency of 10 rad/s and a strain amplitude of 0.001%.

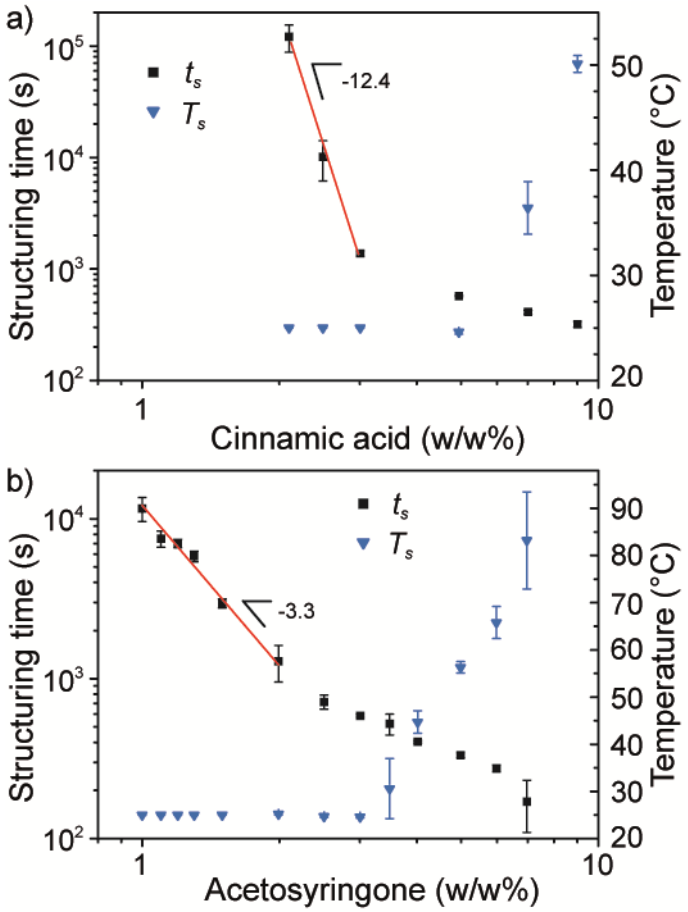

Figure 4 – Structuring kinetics: Structuring time t_s (■, left y axis) and temperature T_s (▼, right y axis) of the organogels versus mass fraction of cinnamic acid (a) and acetosyringone (b). The red curves are power law fittings of the data below 2% (a) and 3% (b) and the power law exponent is reported. In both graphs, the points represent the average values obtained from three tests and the error bars indicate the amplitude of the values obtained.

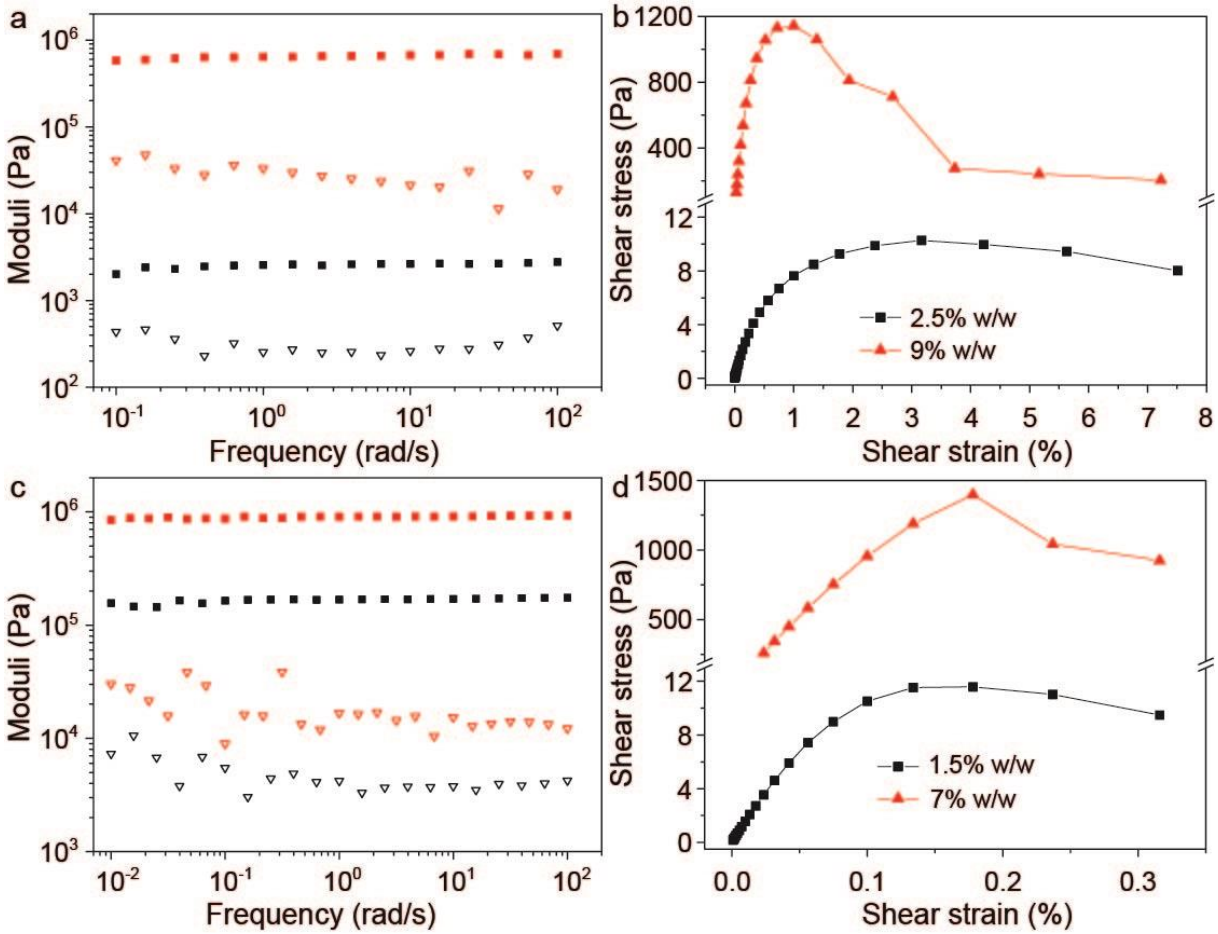

Figure 5 –Linear and non-linear rheology of organogels : Frequency sweep (a) and shear stress curve vs. shear strain (b) of organogels made of cinnamic acid in sunflower oil. The storage ((■, ■) and loss (▽, ▽) moduli are shown at a mass fraction of 2.5% (black data) and 9% (red data). Frequency sweep (c) and shear stress curve vs shear strain (d) of organogels of acetosyringone in sunflower oil at the mass fractions of 1.5% (black data) and 7% (red data). Frequency sweep experiments are done at a strain amplitude of 0.01%. Shear stress curves are measured at a frequency of 10 rad/s.

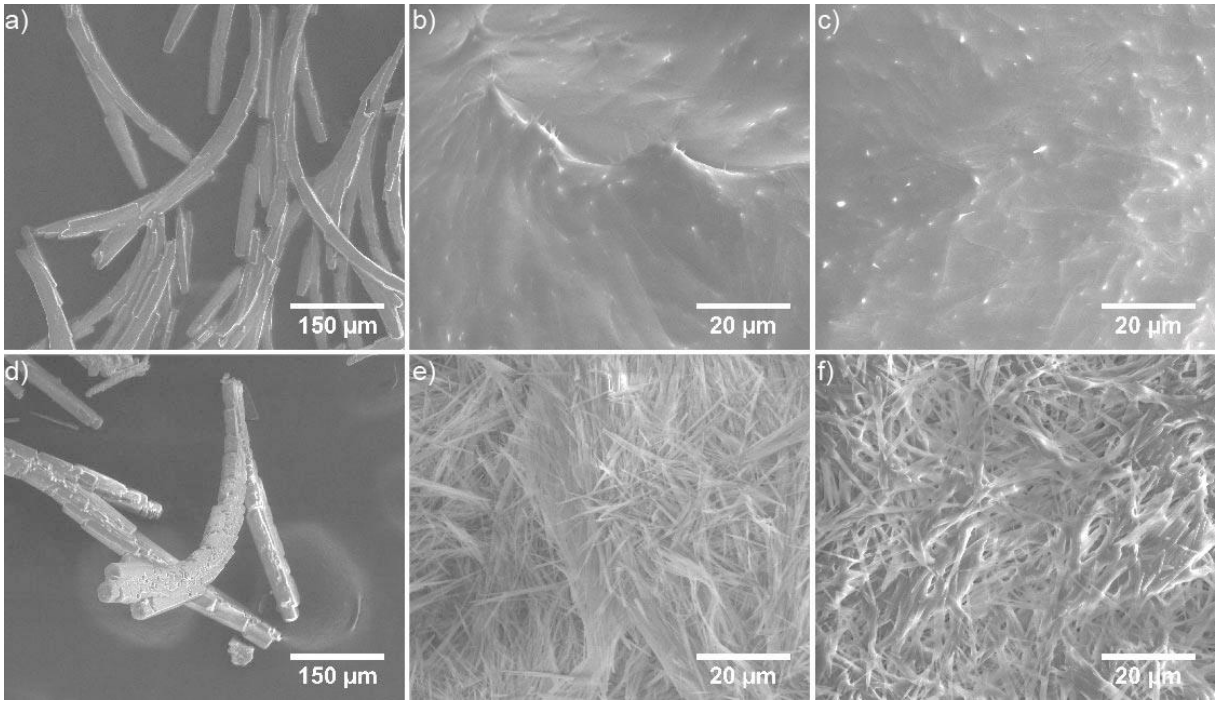

Figure 6 – Wetting of the crystals by sun flower oil : SEM images of the organogel networks of acetosyringone at 1.2% (a, d), 1.5% (b, e) and 3.5% (c, f), obtained in the rheometer. at a cooling rate of 10°C/min. Top micrographs show the organogel network after drainage of oil by suction with a filter paper. Bottom micrographs show the network after rinsing with cyclohexane.

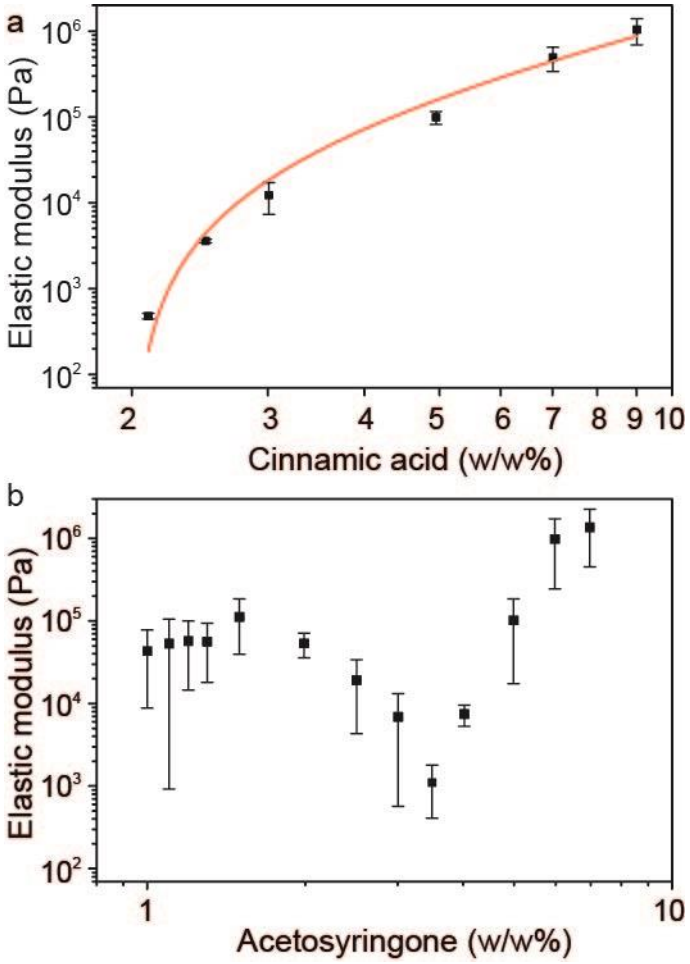

Figure 7 - Elastic modulus versus organogelator mass fraction of the organogels made with cinnamic acid (a) and acetosyringone (b). The modulus is obtained at a frequency of 10 rad/s and a strain of 0.001%. In (a) the red curve is a nonlinear regression of the data according to the equation $G' = A (\Phi - \Phi_0)^{\alpha}$ imposing a critical mass fraction Φ_0 equal to 2%. In (a) and (b), each point represents the average value of three gelation tests and the error bars indicate the minimum and maximum value.

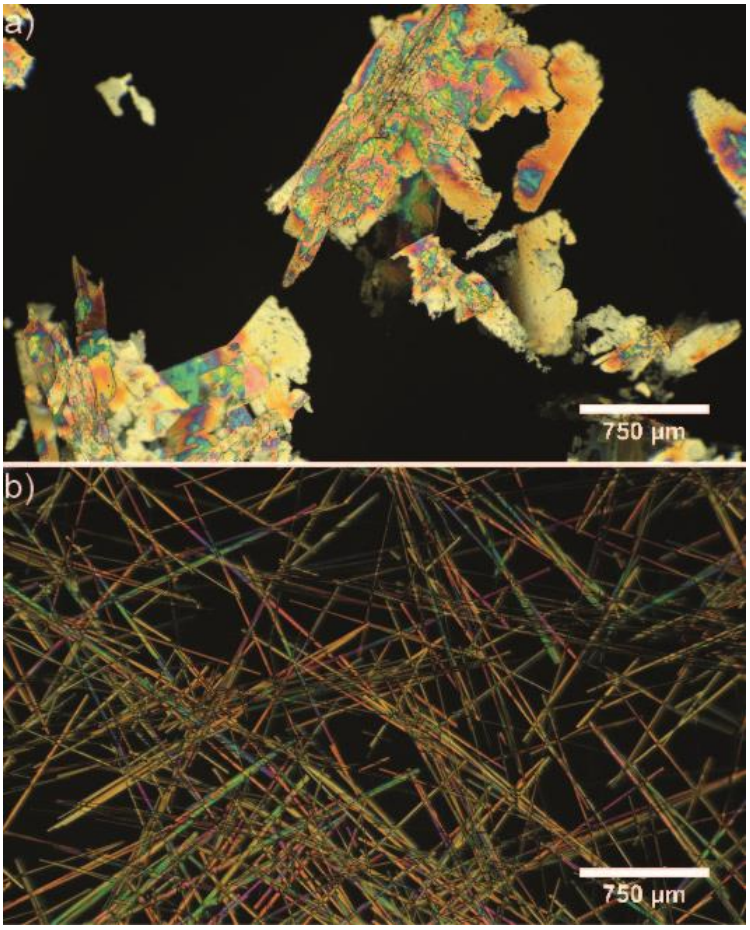

Figure 8 – Optical microscopy images under crossed polarizers of crystals of cinnamic acid (a) and acetosyringone (b) slowly recrystallized in a vial at 3%w/w in sunflower oil.

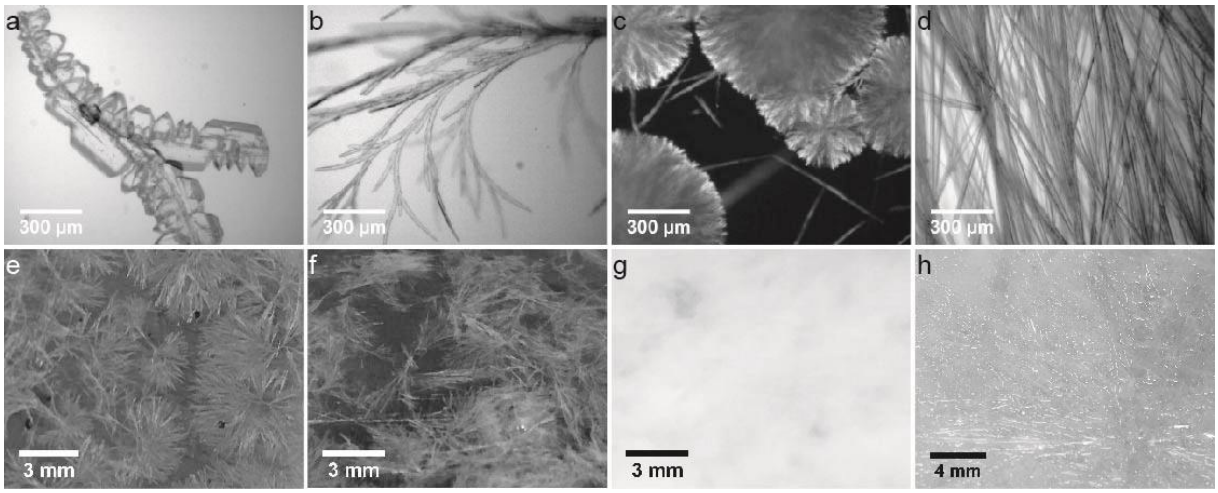

Figure 9 – : Evolution of the morphology of acetosyringone crystals as mass fraction increases : 1.2% (a, e), 1.5% (b, f), 3.5% (c, g) and 7% (d, h). Top images are recorded with an optical microscope and bottom images with a smartphone camera. Image c is taken under crossed polarizers.

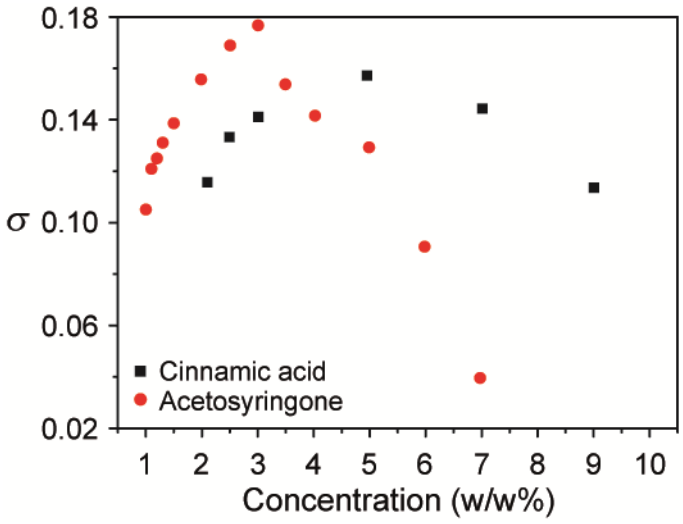

Figure 10 – Parameter σ vs organogelator mass fraction for oleogels obtained at a cooling rate of 10°C/min. σ characterises how far from equilibrium condition the structuring process took place.

Supporting information

1. Kinetics of structuring sunflower oil by recrystallization of cinnamic acid and acetosyringone

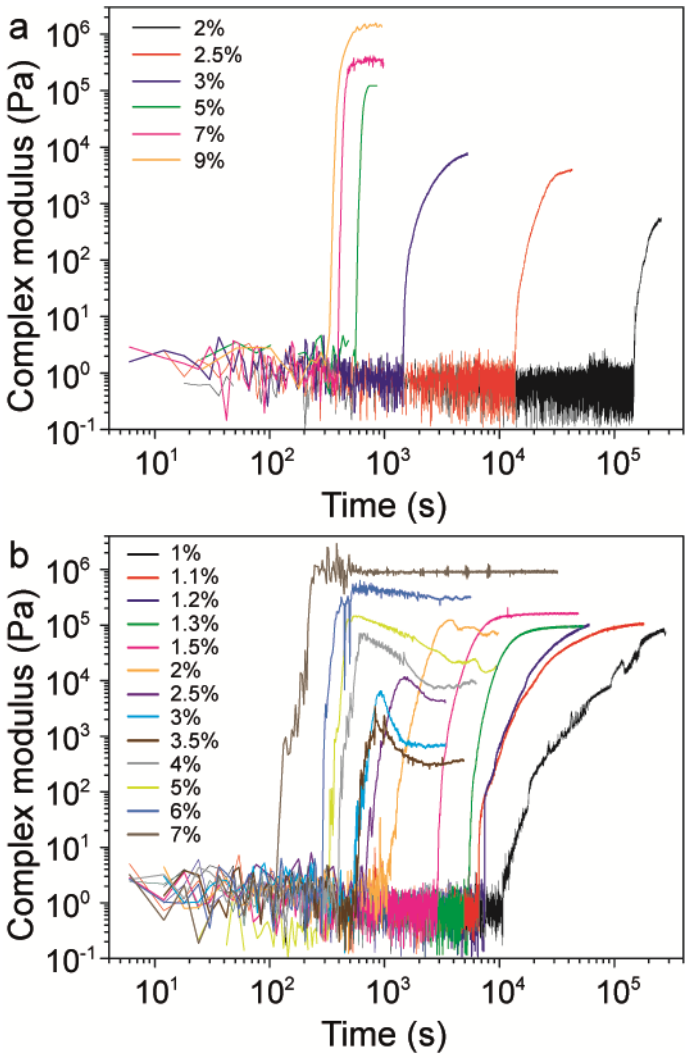

Figure SI 1 - Complex modulus G versus time, upon cooling at 10°C/min, at several concentrations of cinnamic acid (a) and acetosysringone (b). The moduli are measured at a frequency of 10 rad/s and a strain amplitude of 0.001%.*

2. Kinetics of structuring : Illustration of correlation effect due to dilution

The gelation process involves both the growth of the crystals and their aggregation. Crystals growth leads to dense ordered objects represented as black squares in Figure SI2. Aggregation leads to disorded tenuous objects. Both process result from the work of attractive interactions between the molecules of gelator, but kinetic effects determine the configuration of established contact.

If all the molecules would condense in a well packed single crystal, the crystallization of the phenolic compound would not lead to gelation but to a single piece of solid as in Figure SI2a. Gelation occurs only if crystallization is limited to small scales so that the building units of aggregation process, the crystallites, are numerous enough for the solid content to span the entire volume as in Figure SI2 c and d. The relative kinetics of the two processes determine the average size of the crystallites and dilution favors the growth of the crystal.

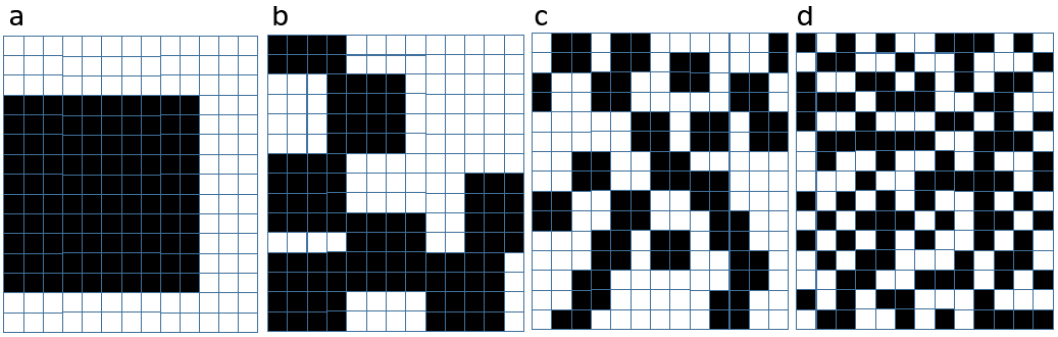

Figure SI2 - Lattice model for oleogelation by crystallization. The gelation process involves both the growth of the crystals and their aggregation. Products of the crystalline growth correspond to squares, while aggregation leads to randomly ramified clusters. The various lattices show that less effective volume is occupied when crystals are larger.

30

3. Crossover from linear to non-linear regime: Log-log representation of the strain amplitude dependence of G' and G".

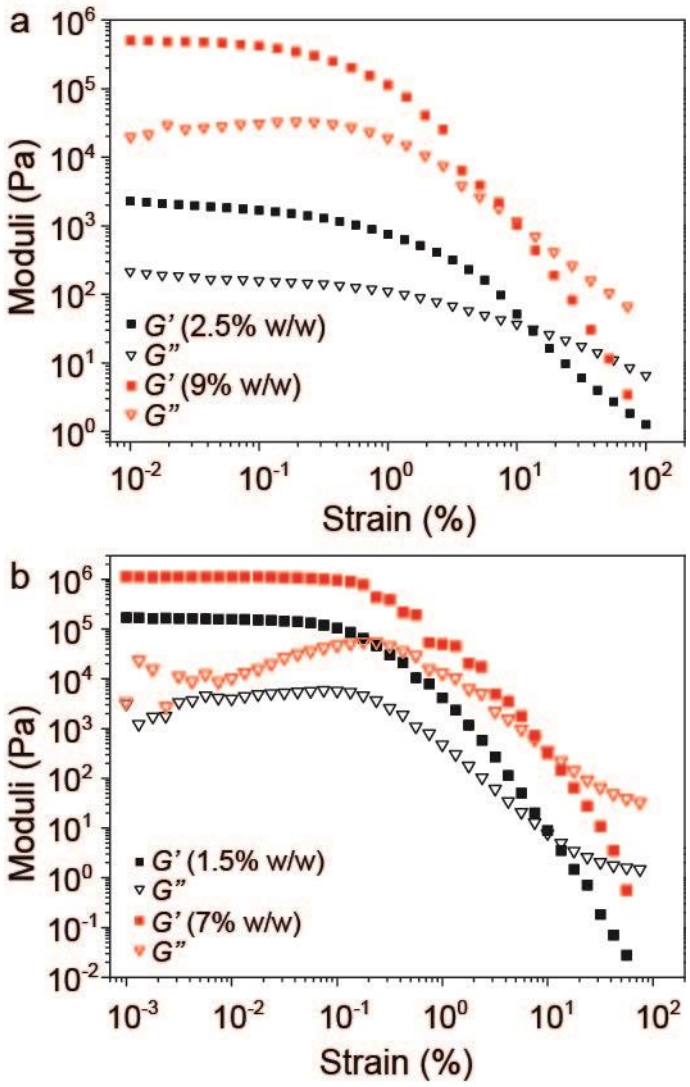

35 *Figure SI 3 - Amplitude sweep of cinnamic acid (a) and acetosyringone (b) organogels at two different concentrations. Black data report the lowest concentration while red data show the highest. The test is done at a frequency of 10 rad/s.*

4. Morphology of cinnamic acid crystals

4.1. Optical texture of cinnamic acid based oleogels

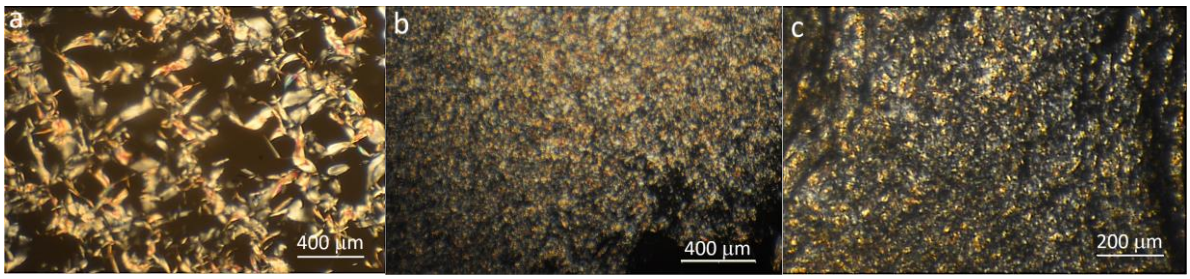

Figure SI 4 - Optical texture of the oleogels of Cinnamic acid in sunflower oil at various cinnamic acid content : (a) 2%, (b) 4% and (c) 8%. The oleogels have been formed between glass slide et cover slip 150µm apart, at a cooling rate of about 8°C/min as explained in section 2.4 of the main text.

4.2. Scanning electronic microscopy of the crystallites

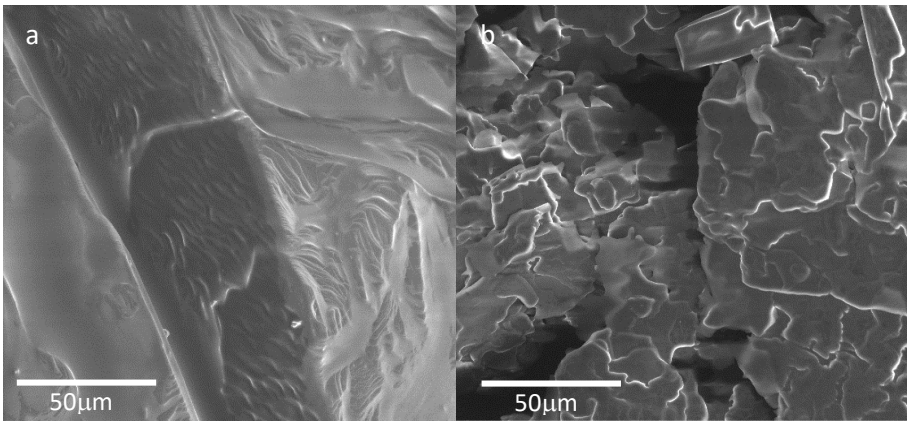

Figure SI 5 - Wetting of the crystals by sun flower oil : (a) SEM images of the crystallites of cinnamic acid extracted by filtration from the organogel obtained at 7% under rheological testing. (b) SEM images of the crystallites of cinnamic acid extracted by filtration and rincing from the organogel obtained at 9% under rheological testing.

5. Evidence for secondary nucleation events

The morphology of the crystal at large scale is characterized by curvature and branching, both resulting from secondary nucleation and subsequent growth. On Figure SI 2 several straight rods with hexagonal cross section are observed on top of each other. The concomitant growth of adjacent rods leads to a branching point. When the growth of one of the rod stops, the slightly different orientation of the rods leads to a curvature at large scale.

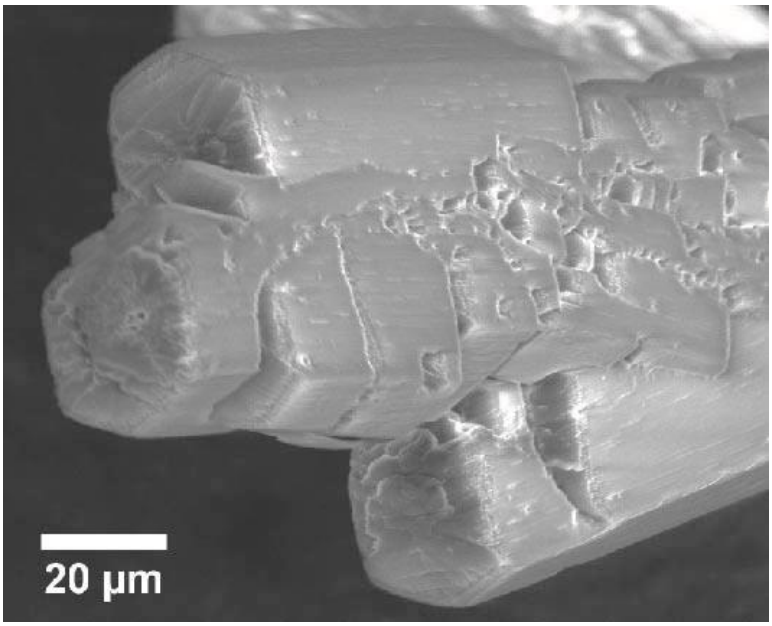

Figure SI 6 - SEM image of an acetosyringone crystal at 1.2% of acetosyringone.